ENVIRONMENTAL RESEARCH
LETTERS

LETTER • OPEN ACCESS

Increasing interannual variability of global vegetation greenness

To cite this article: Chen Chen *et al* 2019 *Environ. Res. Lett.* **14** 124005

Environmental Research Letters

LETTER

Increasing interannual variability of global vegetation greenness

Chen Chen[1], Bin He[1], Wenping Yuan[2], Lanlan Guo[3] and Yafeng Zhang[1]

[1] State Key Laboratory of Earth Surface Processes and Resource Ecology, College of Global Change and Earth System Science, Beijing Normal University, Beijing 100875, People's Republic of China
[2] School of Atmospheric Sciences, Sun Yat-Sen University, Guangzhou, People's Republic of China
[3] Academy of Disaster Reduction and Emergency Management, School of Geography, Beijing Normal University, Beijing 100875, People's Republic of China

E-mail: Hebin@bnu.edu.cn

Keywords: vegetation greenness, increase, global, interannual variability

Supplementary material for this article is available online

OPEN ACCESS

RECEIVED
1 February 2019

REVISED
14 October 2019

ACCEPTED FOR PUBLICATION
22 October 2019

PUBLISHED
19 November 2019

Abstract

Despite the long-term greening trend in global vegetation identified in previous investigations, changes in the interannual variability (IAV) of vegetation greenness over time is still poorly understood. Using Global Inventory Modeling and Mapping Studies normalized difference vegetation index (NDVI) third generation data and corresponding meteorological data from 1982 to 2015, we studied the changes and drivers of the IAV of vegetation greenness as indicated by the coefficient of variation of vegetation greenness at a global scale. Dry and high-latitude areas exhibited high NDVI variability whereas humid areas exhibited relatively low NDVI variability. We detected an increase in the global IAV of vegetation greenness over time using a 15 year moving window. Spatially, we observed significant increases in the IAV of vegetation greenness in greater than 45% of vegetated areas globally and decreases in 21%. Our comparison of ecological models suggests good performance in terms of simulating spatial differences in vegetation variability, but relatively poor performance in terms of capturing changes in the IAV of vegetation greenness. Furthermore, the dominant climate variables controlling changes in the IAV of vegetation greenness were determined spatially using principal component regression and partial least squares regression. The two methods yielded similar patterns, revealing that temperature exerted the biggest influence on changes in the IAV of vegetation greenness, followed by solar radiation and precipitation. This study provides insights into global vegetation variability which should contribute to an understanding of vegetation dynamics in the context of climate change.

1. Introduction

Terrestrial ecosystems are important global carbon sinks that can offset a substantial proportion of anthropogenic CO_2 emissions (Beer *et al* 2010, Pan *et al* 2011, Reichstein *et al* 2013, Ahlström *et al* 2015a). Terrestrial vegetation strongly regulates atmospheric CO_2 concentrations in terms of accumulation, seasonality, and interannual variability (IAV) (Keenan *et al* 2016, Yuan *et al* 2018). Hence, monitoring the drivers of ecosystem dynamics is crucial for forecasting future climate change.

Satellite observations reveal a greening trend on Earth's surface since the 1980s (Zhu *et al* 2016). However, this does not necessarily indicate that greening improves ecosystem functioning because long-term averages ignore IAV which is a critical indicator of ecosystem vulnerability or resilience to external disturbances (Thornton *et al* 2014, Smith *et al* 2014, Ray *et al* 2015, Sloat *et al* 2018). Low IAV in vegetation greenness indicates that vegetation growth is stable and not easily disturbed by external factors (Thornton *et al* 2014), whereas high IAV indicates unstable vegetation growth that has undergone large disturbances and remains vulnerable to future disturbance. For example, low IAV of crop yields indicates that food supplies and farm incomes are stable (Reidsma *et al* 2010, Ray *et al* 2013). In ecosystems, indicators of

vegetation greenness and ecosystem production have been used to study IAV (Ahlström *et al* 2015a, Zhang *et al* 2016, Jiang *et al* 2017, Hu *et al* 2018), but it is unclear how IAV changes over the long term. A global survey of how the IAV of ecosystem productivity changes over time is critical for deepening our understanding of ecosystem resilience to climate change.

Climate change is expected to trigger more frequent climate extremes, including droughts and heatwaves (IPCC 2013). Such changes in climate variability can have profound impacts on ecosystem productivity (Smith *et al* 2014). Ray *et al* (2015) analyzed the effects of climate variability on crop yields and found that one-third of global crop yield variability could be explained by climate variability. Le Hourou *et al* (1988) found that precipitation variability influences variability in ecosystem productivity. Sloat *et al* (2018) found an increasing influence of precipitation variability on productivity in grazing lands globally. However, it is presently unclear how the IAV of ecosystem productivity responds to climate change.

Here, we used the satellite-based normalized difference vegetation index (NDVI) (Rouse *et al* 1973) as a proxy for ecosystem productivity to examine temporal-spatial patterns in IAV from 1982 to 2015 and explored the potential climatic drivers of the IAV of vegetation greenness.

2. Materials and methods

2.1. Data sets

The NDVI is typically used to detect vegetation greenness. Here we used the Global Inventory Modeling and Mapping Studies (GIMMS) NDVI third generation data for the time series 1982–2015, which has a spatial resolution of 1/12 degree and a temporal resolution of 15 d. The maximum value composite (MVC) method (Holben 1986) was adopted to aggregate the biweekly data into monthly intervals. This method can largely remove the contaminations of cloud and atmospheric noises (Holben 1986). Barren regions with an annual mean NDVI less than 0.1 were excluded from the analysis (Piao *et al* 2005, Chen *et al* 2018).

Climate data from the Climatic Research Unit (CRU) Time Series 4.01 with a 0.5° resolution of monthly temperature (TMP) and precipitation (PRE) from 1901 to 2016 were used in this study (Harris *et al* 2014). Monthly shortwave radiation (SWD) data with a resolution of 0.5° was obtained from the CRU-National Centers for Environmental Prediction (CRU-NCEP) v7 data set.

To evaluate the performance of different Dynamic Global Vegetation Models (DGVMs) in capturing the IAV of vegetation growth, we compared gross primary productivity (GPP) simulations from eight DGVMs archived in the Trends in Net Land-Atmosphere Exchange (TRENDY-v6) project from 1982 to 2015 with observations of NDVI variability (Sitch *et al* 2015). We selected the following eight ecological models: CABLE, DLEM, ISAM, LPJ-wsl, OCN, ORCHIDEE, VEGAS, and VISIT.

In addition, global land cover data with a spatial resolution of 0.05° was obtained from MODIS Land Cover Climate Modeling Grid (MCD12C1) Version 6 from 2001 to 2015. We used the International Geosphere and Biosphere Programme land cover classifications to select nine biomes (figure S1(a) is available online at stacks.iop.org/ERL/14/124005/mmedia and table S1), including evergreen needleleaf forests (ENF), deciduous needleleaf forests (DNF), evergreen broadleaf forests (EBF), deciduous broadleaf forests (DBF), mixed forests (MF), savannas, shrublands, grasslands, and croplands. We used only areas (pixels) with a constant vegetation type from 2001 to 2015 to prevent land cover changes from impacting our results.

Global climate zones were determined based on Köppen–Geiger classifications (Kottek *et al* 2006) obtained from http://koeppen-geiger.vu-wien.ac.at/. We focused on five major climate zones: equatorial, arid, warm temperate, snow, and polar, as shown in figure S1(b) and table S2. Previous investigations have suggested great difference in vegetation behavior under different climate zones (Liu *et al* 2013, Iio *et al* 2014, Ahlström *et al* 2015b).

The above data sets comprise different time series, so we limited our analysis to the time period from 1982–2015 to match the NDVI series. Furthermore, all datasets were further aggregated to 0.5° × 0.5° using nearest neighbor resampling technique to match the resolution of the climate data sets (Knorn *et al* 2009, Zhu *et al* 2013, Gatti *et al* 2017).

2.2. Methods

2.2.1. Coefficient of variation

Here, we used the coefficient of variation (CV) of NDVI ($NDVI_{\_CV}$) and the CV of GPP ($GPP_{\_CV}$) to represent in the IAV of vegetation growth (Fang *et al* 2001, Schucknecht *et al* 2013, Sloat *et al* 2018). CV is an absolute value that measures the degree of dispersion of a variable. Its size is affected not only by the degree of variable dispersion, but also by the average of the variable's value. The formula is generally expressed as:

$$CV = (SD/MN) \times 100\%, \quad (1)$$

where, SD represents the standard deviation and MN represents the mean of the studied variables.

Both the annual growing season and annual maximum NDVI_cv were determined here.

To test the sensitivity of CV of studied variable to SD and MN, a simple linear regression (Yang *et al* 2016) of CV against SD and MN was performed. The sensitivity was determined according the slope of CV to SD and MN, and a larger slope indicates a higher sensitivity.

2.2.2. Land surface phenology

Various methods have been developed for retrieving phenological dates from NDVI data, such as HANTS-Maximum (Jakubauskas *et al* 2001), Polyfit-Maximum (Piao *et al* 2015), Savitzky–Golay filter (Zhu *et al* 2016), double logistic (Julien and Sobrino 2009), and others. Here, the growing season for land plants was determined from the GIMMS NDVI3g data set using a Savitzky–Golay filter that effectively smoothed the original curve and somewhat reduced the noise in the time series data (Chen *et al* 2004, Jönsson and Eklundh 2004, Cong *et al* 2012). Figure S2 shows the global patterns in surface phenology from 1982 to 2015, average start day and length of the growing season.

2.2.3. Mann–Kendall (MK) statistical test

To study the dynamics of $NDVI_{\_CV}$ and $GPP_{\_CV}$, we applied a 15 yr moving time window to the NDVI/GPP sequence from 1982 to 2015. A CV value representing the IAV of vegetation growth over a specific 15 yr period was calculated and assigned to the middle year of each window. This approach generated a series of 20 CV values with the first value representing the first 15 yr period from 1982 to 1996 and the 20th CV value representing the last 15 yr period from 2001 to 2015. The trend in window position values was detected using the Mann–Kendall (MK) non-parametric test method (Mann 1945). The advantage of the method is that the series does not need to follow a specific distribution and is seldom disturbed by abnormal values, so the calculation is straightforward and convenient (Hamed 2008). We applied the trend-free pre-whitening technique to the studied time series (Yue *et al* 2002, Erasmi *et al* 2014) before performing the trend test because the autocorrelation in the time series has been found to influence the significance of the Mann–Kendall trend test (Yue *et al* 2002). The strength of the time series trend was estimated using the Theil–Sen method (Fensholt *et al* 2012, Schucknecht *et al* 2013). This trend estimator calculates the slope of every single data pair in a time series and uses the median slope to characterize a trend in the data (Sen 1968). The significance of the CV trend was assessed at a p-value less than 0.05. In addition, we also examined $NDVI_{\_CV}$ trends determined from 11, 13, 17, and 19 yr windows to test the potential influence of window length on our results.

2.2.4. Principal component regression (PCR) and partial least squares regression (PLSR)

Several factors were selected to explore the drivers of $NDVI_{\_CV}$, including the mean values of climate variables ($TMP_{\_mean}$, $PRE_{\_mean}$, and $SWD_{\_mean}$) and the CVs of climate variables ($TMP_{\_CV}$, $PRE_{\_CV}$, and $SWD_{\_CV}$) corresponding to each 15 yr window. Regression analysis between $NDVI_{\_CV}$ and the six potential drivers were performed to determine the main drivers. To reduce the uncertainty caused by the analysis method, two regression methods, the principal component regression (PCR) and the partial least squares regression (PLSR), were used in this study. Compared with traditional multivariate linear regression, these two methods can effectively overcome the multicollinearity problem existing among two or more explanatory variables. PCR is based on principal component analysis (Jolliffe 1982), which decomposes explanatory variables into several principal components. Instead of regressing the original dependent variable on the explanatory variables directly, the principal components of the explanatory variables are used for regression analysis (Jolliffe 1982). The PLSR is similar to PCR in that it integrates the basic functions of multiple linear regression analysis, canonical correlation analysis, and principal component analysis (Chun and Keleş 2010, Mehmood *et al* 2012). Variable importance in the projection (VIP) is the PLSR standard for judging the importance of independent variables in modeling. When VIP is greater than or equal to 1, its corresponding independent variables have strong explanatory significance to the dependent variables (Chong and Jun 2005). All variables were standardized before calculation.

We noted that data processing was performed in MATLAB 2014a environment, and global maps were drawn using ArcGIS 10.3.

3. Results

3.1. Global pattern of variability of vegetation greenness

Figure 1(a) shows the spatial distribution of the IAV of NDVI ($NDVI_{\_CV}$) from 1982 to 2015. $NDVI_{\_CV}$ demonstrates high spatial heterogeneity. We observed relatively low IAV of vegetation greenness in the equatorial and snow climate zones (figures 1(b), S1), including tropical rainforests near the equator and boreal forests between 50° and 60 °N latitude. In contrast, we observed high CV values in the vegetated lands of arid and polar climates zones, including western and southwestern Asia, Australia, northern and southern Africa, southwestern North America, and areas above 60 °N. At the biomes scale (figure 1(c)), evergreen broadleaf forests exhibited the lowest IAV of vegetation greenness, whereas grasslands demonstrated the highest IAV.

3.2. Dynamics of variability of vegetation greenness

The trend of $NDVI_{\_CV}$ sequences generated from the 15 yr moving window from 1982 to 2015 was detected for each grid cell, as shown in figure 2. Significant vegetation IAV, indicated by annual maximum NDVI (figure 2(a)) decreases, were observed in more than 21% of vegetated lands scattered across Europe, the Indian peninsula, the sahel region, the southwest of America and the north of Asia. This indicates increasing stability of local ecosystems. Simultaneously,

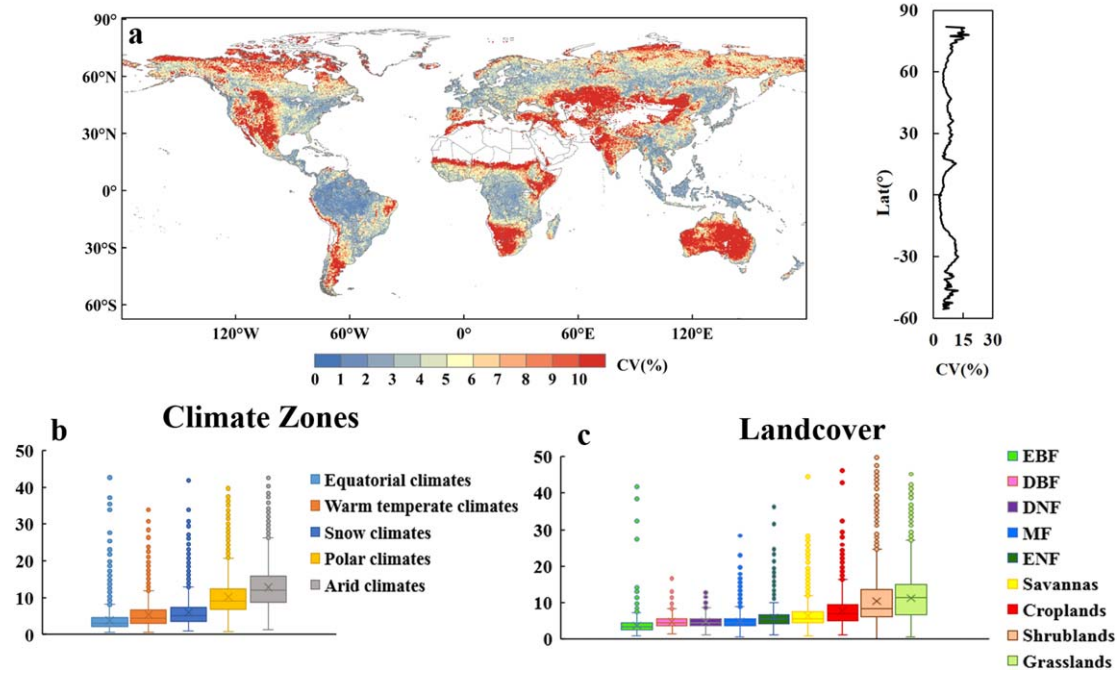

Figure 1. (a) Spatial pattern of the NDVI coefficients of variation (CV) for the period 1982–2015. The box plots indicate the CV of NDVI for the period 1982–2015 for (b) different climatic zones and (c) different vegetation types. Five major climate groups were determined based on Köppen–Geiger climate classification: equatorial, arid, warm temperate, snow, and polar. Nine vegetation types were determined using the MODIS Land Cover Climate Modeling Grid (MCD12C1) Version 6: evergreen needleleaf forests (ENF), deciduous needleleaf forests (DNF), evergreen broadleaf forests (EBF), deciduous broadleaf forests (DBF), mixed forests (MF), savannas, shrublands, grasslands, and croplands.

significant increases in vegetation variability occurred in northeastern China, western Asia, the southwestern United States, much of Australia, and central Africa, accounting for more than 45% of vegetated areas globally. The trend in growing season $NDVI_{\_CV}$ (figure 2(b)) roughly agreed with that of annual maximum $NDVI_{\_CV}$. We observed decreases in growing season $NDVI_{\_CV}$ in 30% of vegetated areas and increases in 40% of vegetated areas globally. Figure 2(c) shows the probability density function of the trends in annual maximum $NDVI_{\_CV}$ and growing season $NDVI_{\_CV}$. We observed a higher proportion of increases than decreases. In addition, growing season $NDVI_{\_CV}$ demonstrated more increasing trends than did annual maximum $NDVI_{\_CV}$. Note that the $NDVI_{\_CV}$ trends determined using different moving time windows present a similar pattern with that of the 15 yr window (figure S3), suggesting a basic reliability of $NDVI_{\_CV}$ change built here.

$NDVI_{\_CV}$ changes can be caused by variations in standard deviation or the mean value of NDVI, so we examined trends in these two values and tested the sensitivity of $NDVI_{\_CV}$ to them (figure S4). The mean values of annual maximum NDVI displayed increasing trends in most regions (figure S4(a)), with decreasing trends in northeast China, the northern of North America, and the Congo rainforest. Trends in NDVI standard deviation were similar to those of $NDVI_{\_CV}$ (figure S4(b)). Sensitivity tests suggest that $NDVI_{\_CV}$ was more sensitive to the standard deviation of NDVI than to the mean value of NDVI in nearly all continents (figure S4(c)), suggesting that standard deviation exerted a dominant influence over $NDVI_{\_CV}$ trends.

We further explored trends in regional mean annual maximum $NDVI_{\_CV}$ by dividing global vegetated lands into different regions (figure 3). Global mean $NDVI_{\_CV}$ demonstrated a significant increasing trend and the slope of $NDVI_{\_CV}$ in the Southern Hemisphere (SH) was larger than that in the Northern Hemisphere (NH). For different climate zones, the largest increase in $NDVI_{\_CV}$ was observed in the vegetated lands of polar and arid climate zones. In contrast, vegetation in humid and warm temperate climate zones presented the lowest increase in variability. At the biome scale, significant increases in $NDVI_{\_CV}$ were found for the majority of vegetation types, including shrublands, grasslands, evergreen broadleaf forests, deciduous needleleaf forests, and savannas. Simultaneously, $NDVI_{\_CV}$ exhibited decreasing trends in mixed forests and croplands, but the trends were not statistically significant.

3.3. Performance of ecosystem models in simulating vegetation variability

To examine whether the observed IAV of vegetation growth can be captured by ecological models, we studied the $GPP_{\_CV}$ simulated from TRENDY-models

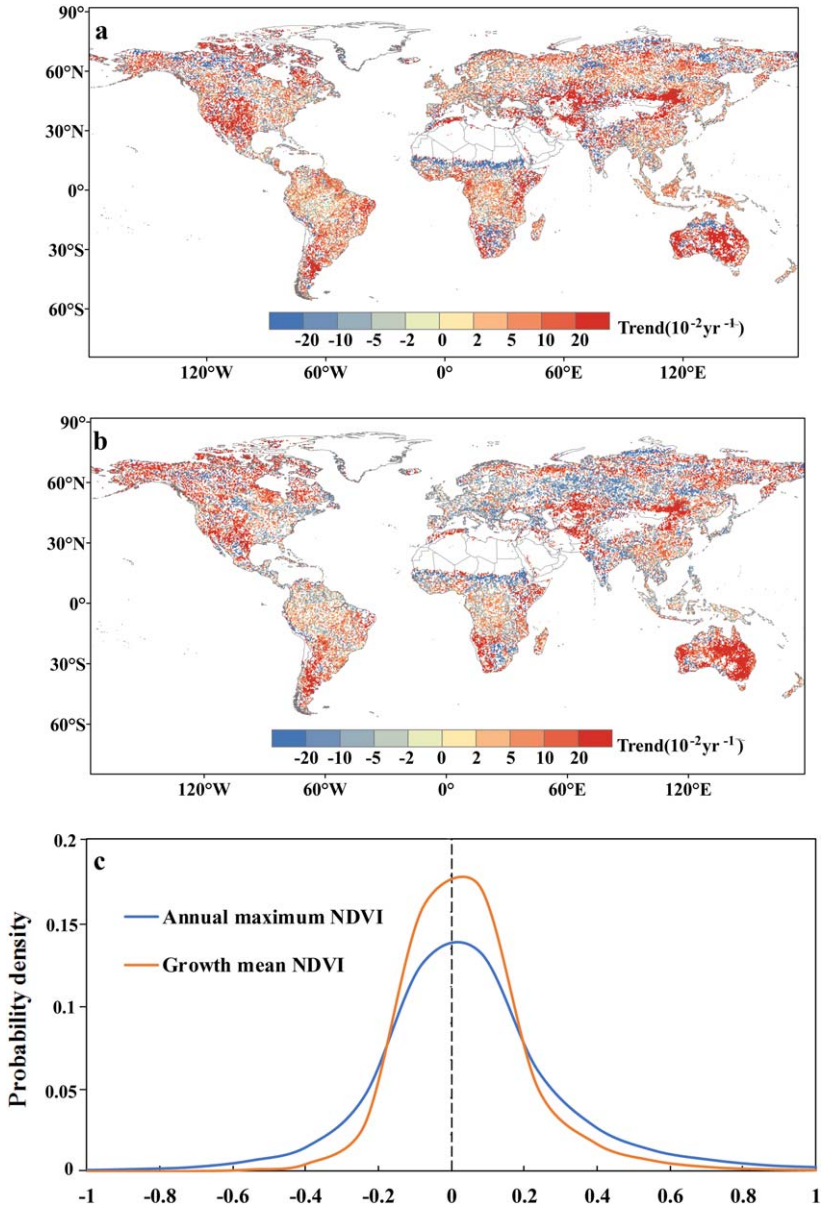

Figure 2. Spatial pattern of significant trends (Mann–Kendall test, $p < 0.05$) in (a) annual maximum NDVI$_{_CV}$ and (b) growing season NDVI$_{_CV}$ estimated using a 15 yr moving window from 1982 to 2015. (c) The probability density function of NDVI$_{_CV}$ trends for annual maximum value and growing season value.

(figure 4). The spatial pattern of modeled GPP$_{_CV}$ from 1982 to 2015 (figure 4(a)) agreed well with the distribution of NDVI$_{_CV}$ (figure 1(a)), producing high CV values in drier regions and low values in humid and high-latitude regions. We further examined the patterns of GPP$_{_CV}$ determined using a 15 yr moving widow, as shown in figure 4(b). The models only partially reproduced the spatial patterns of NDVI$_{_CV}$ trend (figures 2(a) and (b)), including the increasing CV in northeastern China, western Asia, southern North America, and the Congo. However, opposite trends were observed in northern Asia, eastern Europe, and northern Australia, suggesting that the performance of current ecosystem models in modelling the IAV of vegetation growth still needs to be improved.

3.4. Drivers of variability of vegetation greenness

To explore the drivers of NDVI$_{_CV}$, we first examined the partial correlations between NDVI$_{_CV}$ and climate variability and mean state over different periods (figure S5). There was a strong positive correlation between TMP$_{_CV}$ and NDVI$_{_CV}$ in Europe and Australia, and a large continuous negative correlation in southern North America, central South America, and southwestern and northeastern Asia. TMP$_{_mean}$ presented more extensive positive impacts on NDVI$_{_CV}$ (22% of global vegetated lands) than did TMP$_{_CV}$ (16% of global vegetated lands), mainly concentrating in relatively humid regions such as the eastern South America, southern China, and the Congo rainforest. Negative impacts between TMP$_{_mean}$ and NDVI$_{_CV}$ were also observed over

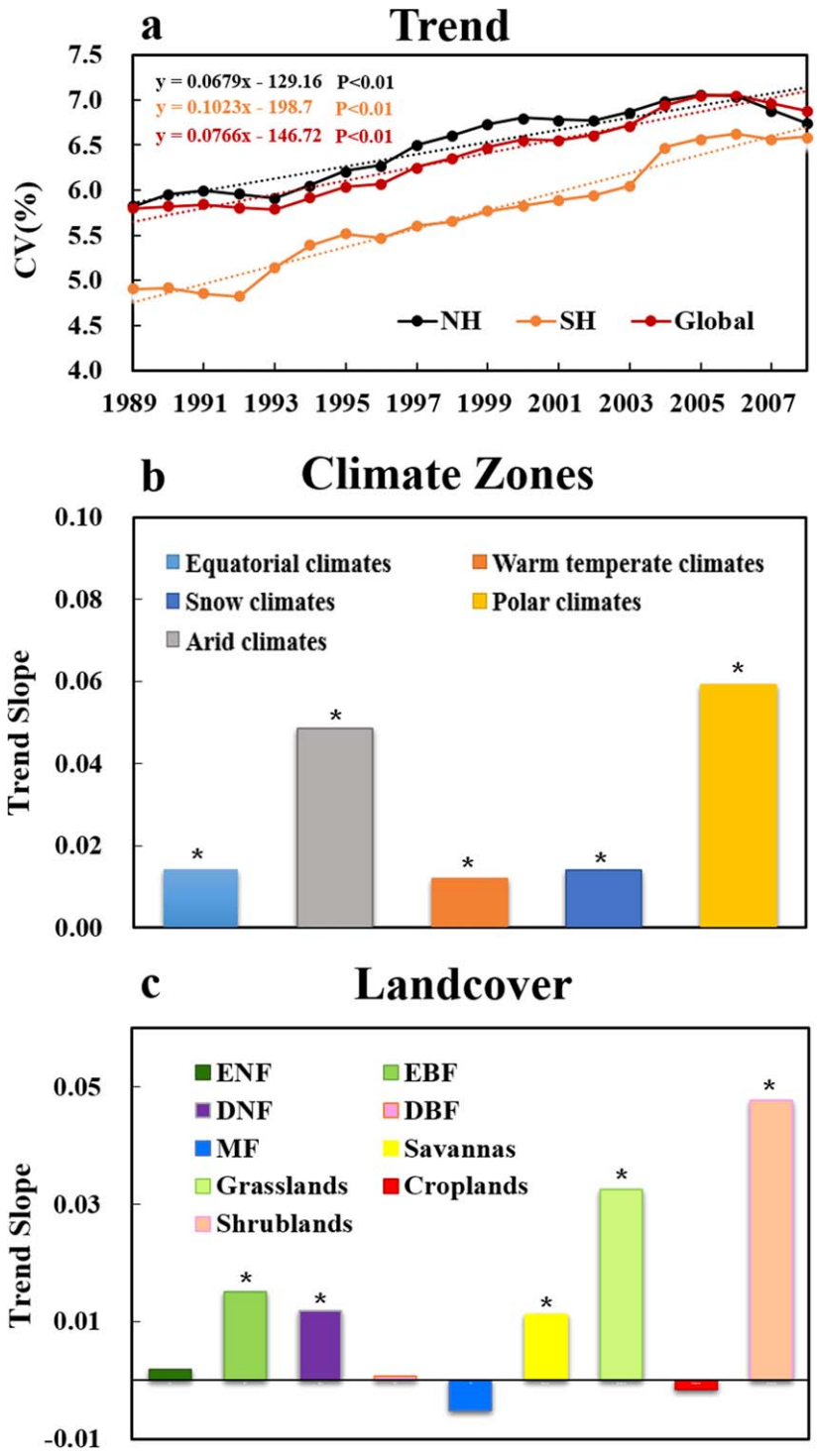

Figure 3. Trends in NDVI_CV over time (a) in the Northern Hemispheric (NH), Southern Hemisphere (SH), and the global mean after applying 15 yr moving windows; (b) trends in mean NDVI_CV in different climate zones; (c) trends in mean NDVI_CV in different land cover types. '*' indicates statistical significance (Mann–Kendall test; $p < 0.05$).

17.3% of global vegetated areas, such as Europe and the Amazon rainforest. We found that PRE_CV exerted a strong positive influence on NDVI_CV for 20.5% of global vegetated lands, whereas PRE_mean exerted a strong negative influence for 19.1% of global vegetated lands. The influences from precipitation were scattered over both arid and humid regions. SWD_CV exerted a comparable negative influence on NDVI_CV (18.8% of global vegetated lands) with a positive influence (17.8% of global vegetated lands); but the SWD_mean had more positive impacts on NDVI_CV than negative impacts. Generally speaking, climate mean states had more extensive impacts on NDVI_CV than did climate variability. In addition, all factors except PRE_mean and SWD_CV exerted more positive than negative impacts on NDVI_CV.

Next, PLSR and PCR were used to determine which climate factors had the strongest effects on the

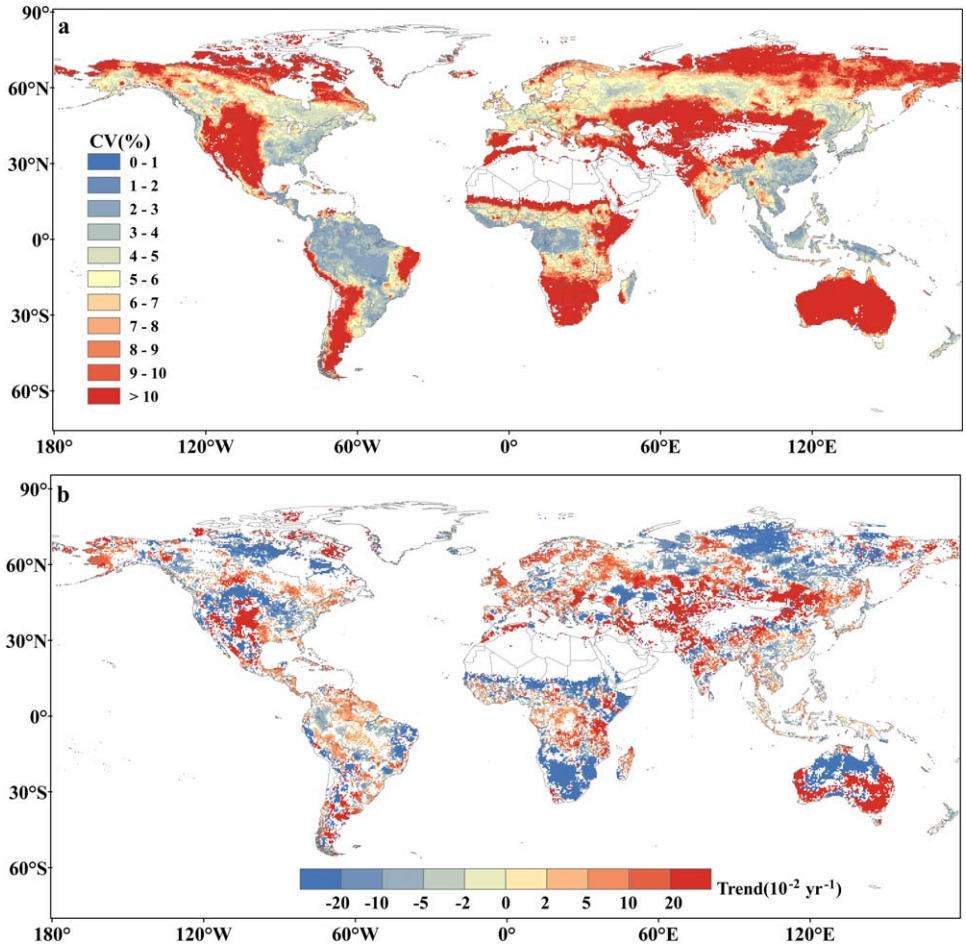

Figure 4. Pattern of GPP_cv averaged from outputs of TRENDY-models. (a) Global pattern of the CV of GPP simulated from TRENDY-models for the period 1982–2015; (b) Pattern of significant trends of the CV of GPP simulated from TRENDY-models after pre-whitening (Mann–Kendall test; $p < 0.05$). We used mean GPP averaged from simulations by eight ecological models from TRENDY-models: CABLE, DLEM, ISAM, LPJ-wsl, OCN, ORCHIDEE, VEGAS, and VISIT. The trends were determined using a 15 yr moving window.

IAV of vegetation greenness. The two regression methods generated comparable results and similar spatial patterns, as shown in figures 5 and S6. Temperature states exerted the most extensive influence on $NDVI_{\_CV}$, accounting for 36.5% (indicated by PLSR) and 35.5% (indicated by PCR) of global vegetated areas with a stronger influence from $TMP_{\_mean}$ than from $TMP_{\_CV}$. Dominant temperature impacts were observed in southern Asia, eastern and northern North America, northern and central South America, and central Africa. Solar radiation states presented the second largest influence on $NDVI_{\_CV}$ variations, accounting for 34% (by PLSR) and 34.3% (by PCR) of global vegetated lands. These regions were scattered across western Asia, western North America, southern South America, and western Australia. Slightly more regions were controlled by $SWD_{\_mean}$ than by $SWD_{\_CV}$. PRE states dominating $NDVI_{\_CV}$ were identified in 29.5% (by PLSR) and 30.2% (by PCR) of global vegetated lands, including northwest Asia, northern and western Europe, northern North America, and southern Africa. We also determined the climatic factors that most influenced $NDVI_{\_CV}$ variations in each climate zone, as shown in figure S7. We observed large divergences in the factors controlling $NDVI_{\_CV}$ changes in different climate zones. $TMP_{\_mean}$ displayed a dominant positive correlation with $NDVI_{\_CV}$ changes in the equatorial climate zone, but a negative relationship in the snow climate zone. $NDVI_{\_CV}$ changes in the arid climate zone were driven by $PRE_{\_mean}$, by $SWD_{\_CV}$ in the warm temperate zone, and by $SWD_{\_mean}$ in the polar climate zone.

4. Discussion

Vegetation variability greatly impacts ecosystem provisioning services and the global carbon cycle (Nemani *et al* 2003, Wu *et al* 2016, Yuan *et al* 2018). This study examined changes in the IAV of vegetation greenness and explored corresponding climatic drivers on a global scale. Spatially, we observed a clear distribution of the IAV of vegetation greenness associated with patterns of climate zones. Low IAV of vegetation greenness occurred in the equatorial and snow climate zones, whereas high IAV occurred in the vegetated

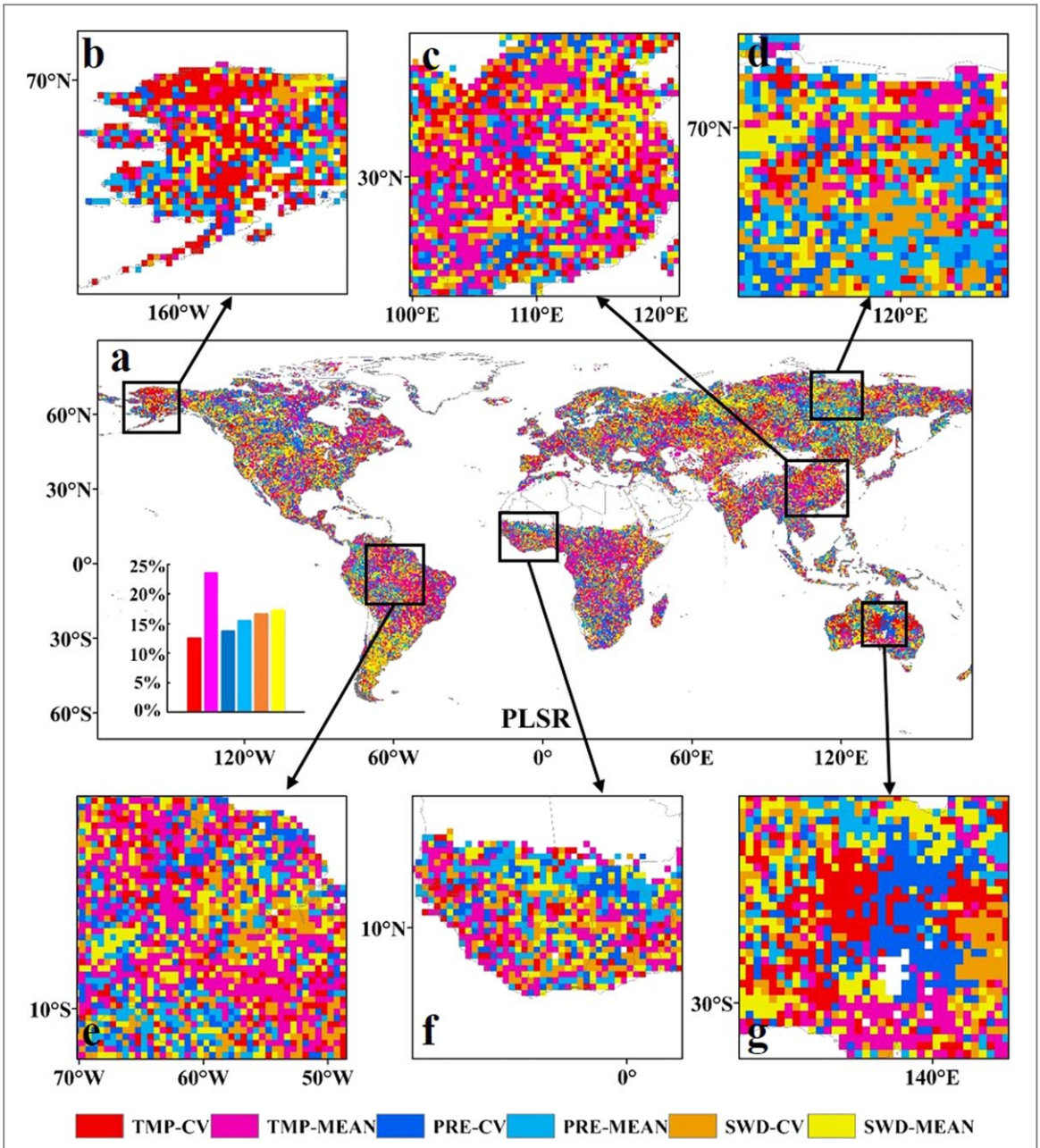

Figure 5. Partial least squares regression (a) of six climatic variables (temperature variability, precipitation variability, solar radiation variability, mean temperature, mean precipitation, and mean solar radiation) with NDVI variability for the period from 1982 to 2015. Six key regions are highlighted: (b) western Alaska, (c) China, (d) a part of Siberia, (e) Amazonia, (f) west Africa and (g) central Australia.

lands of the arid and polar climate zones. This pattern of IAV of vegetation greenness is roughly consistent with previous studies (Zhao *et al* 2018). At the biome scale, the IAV of vegetation greenness in grasslands was highest, whereas variability in evergreen broadleaf forests was lowest. Furthermore, nearly all forests displayed relatively low variability, which agrees with previous research (Fang *et al* 2001, Knapp and Smith 2001). The primary reason for this low variability is that forests are more resistant to climate anomalies than other vegetation types (Hirota *et al* 2011). Without considering disturbances from human activities, vegetation variability should be determined primarily by climate conditions (Wu *et al* 2015). In the current study, we also calculated the spatial distributions of climate factor variability (PRE, TMP, and SWD), as shown in figure S8. Temperature variability presents a clear latitudinal distribution, gradually decreasing with decreasing latitude. The distribution of solar radiation variability has great spatial heterogeneity, with high variability in Europe, southern South America, and western Australia, and lowest in the equatorial regions. The distribution of precipitation variability is highly consistent with the pattern of vegetation variability, with high variability in drier regions and low variability in humid regions, suggesting that precipitation variability is a strong determinant of vegetation variability distribution. Previous

studies have suggested a heavy influence of precipitation variability on ecosystem productivity in global pastures (Sloat *et al* 2018). In addition, precipitation extremes were found to determine the distribution of global vegetation extremes (Liu *et al* 2013, Ahlström *et al* 2015a).

In addition to determining the spatial patterns of the IAV of vegetation greenness trends from 1982 to 2015, we also analyzed the dynamics of vegetation variability over the long term. We found increasing variability in global vegetation greenness, suggesting that the IAV of vegetation growth is increasing. This increase in variability of vegetation greenness was found to be mainly due to the increase in the standard deviation other than the mean value of NDVI, implying that the increase variability should not be attributed to the long-term greening over continents (Zhu *et al* 2016). The increasing of IAV essentially indicates a decrease in stability of vegetation growth to external disturbances. According the measures of vegetation stability proposed by earlier studies (Hoover *et al* 2014, De Keersmaecker *et al* 2015, Seddon *et al* 2016), the decrease of stability seems to suggest the decrease in resistance or resilience, or increase in sensitivity of vegetation growth to environment changes. Increases of vegetation variability were mainly observed in the vegetated lands of arid and polar regions. Despite the small proportions of the vegetated lands in arid zones, the arid and semiarid ecosystems have been suggested to heavily influence the IAV of global ecosystem sinks (Poulter *et al* 2014, Ahlström *et al* 2015a, Huang *et al* 2016). Therefore, the observed increase of vegetation variability would be expected to have profound impacts on global carbon cycle. As previous studies have found, vegetation in arid zones and polar regions were more susceptible to disturbances from the external environment (IPCC 2007, Lioubimtseva and Henebry 2009). This also explains the increase in extreme events such as droughts and heat waves in recent years (Perkins *et al* 2012). Propastin *et al* (2010) found that the vegetation classes 'grassland' and 'closed shrubland' exhibited the largest proportion of land area containing both moderate and high vulnerability to the external environment. Similarly, our study demonstrates that grassland and shrub variability increased most severely. Propastin *et al* (2010) also suggested that forest areas were significantly less affected by climate than the other land cover types. The current study confirms these findings by showing that changes in the IAV of growth of evergreen broadleaf forests and deciduous broadleaf forests were the most stable of the vegetation types. Furthermore, despite large uncertainties, satellite NDVI measurements and multi-model estimates of GPP demonstrated a consistent spatial distribution of vegetation variability over the last 34 years. However, we also noted that these TRENDY models did not fully capture the change trend of vegetation variability as NDVI from 1982 to 2015, suggesting a need for improved ecological models. A recent study also suggested that current ecological models underestimate the IAV of global ecosystem production associated with water availability conditions (Humphrey *et al* 2018).

Numerous factors can influence the IAV of vegetation greenness, including fire, deforestation, and land use changes but large scale changes are driven by climatic factors (Osborne and Wheeler 2013). This study reveals the complex influence of climatic factors on the IAV of vegetation greenness dynamics. The most influential impacts on the IAV of vegetation greenness were from temperature, followed by solar radiation and precipitation. Vegetation growth in the northern high latitudes is usually limited by temperature (Nemani *et al* 2003, Seddon *et al* 2016). Interestingly, we observed strong impacts from precipitation and solar radiation on changes in the IAV of vegetation greenness. Piao *et al* (2014) reported a weakening influence of vegetation change on the IAV of vegetation growth in high latitudes due to disturbances from drought and heatwaves. In addition, warming has caused spring to come early in these regions, which may result in increased water demand by plants during the summer months (Buermann *et al* 2013). Hence, precipitation would be expected to exert a stronger influence on the IAV of annual maximum NDVI. We also observed a dominant influence of temperature on changes in the IAV of vegetation growth in areas where radiation is traditionally thought to control vegetation growth such as tropical regions. Previous studies have found a strong coupling between tropical temperature changes and changes in the IAV of atmospheric CO_2 growth rate, and that this coupling was primarily regulated by the influences of temperature changes on tropical ecosystem productivity (Wang *et al* 2013, Wang *et al* 2014). High temperature tends to promote the vapor pressure deficits, which will induce the closure of plant stomata and thereby the reduction of photosynthesis rate and productivity (McDowell and Allen 2015, Sulman *et al* 2016). In addition, some studies have revealed the strong impacts of drought on rainforest productivity (Phillips *et al* 2009, Samanta *et al* 2010, Xu *et al* 2011, Liu *et al* 2018). High temperatures can trigger drought conditions by increasing vapor pressure deficits and increasing evapotranspiration even in normal rainfall conditions (Corlett 2011, Silva *et al* 2013). In some arid regions, such as southern South America, southern Africa, and Australia, precipitation and solar radiation exert a blended influence on changes in the IAV of vegetation greenness. It is easy to understand the large impact of precipitation on changes in the IAV of vegetation growth because water is the main limiting factor for vegetation growth in these regions (Nemani *et al* 2003). A possible explanation for the observed impact of solar radiation on changes in the IAV of vegetation growth in these regions may be that radiation is a primary energy component that influences soil water conditions by changing atmospheric water demand (Dai 2011).

Despite the long-term greening of Earth's surface, the IAV of vegetation greenness is also increasing, which suggests that the stability of ecosystems is decreasing. This change in the IAV of vegetation greenness should have profound impacts on the dynamics of ecosystem carbon sinks. Considering the strong coupling between ecosystem productivity and atmospheric CO_2 concentrations, the atmospheric CO_2 growth rate would also likely be affected (Richardson *et al* 2010, Graven *et al* 2013, Piao *et al* 2017). It should be noted that there are some limitations to this study. First, the uncertainties associated with remote sensing data cannot be ignored. For example, the NDVI has been suggested to suffer from saturation problem in areas with dense vegetation (Morton *et al* 2014). In addition, it may also contain errors produced by the shift or degradation of sensors and by the noise signals from atmosphere and ground (Atzberger *et al* 2013, Jiang *et al* 2013, Zeng *et al* 2013). Second, this study provides only a preliminary investigation of the climatic drivers of changes in the IAV of vegetation greenness, but the mechanisms of these drivers is still unclear. Although this study focused on the role of climate, other factors that influence the IAV of vegetation growth such as fires, land use and CO_2 fertilization, are also important. Therefore, further analysis involving these factors is needed to fully understand the mechanisms behind the IAV of vegetation growth.

5. Conclusions

This study provides insights into global vegetation variability using satellite-based estimates of vegetation greenness for the period 1982–2015. On a global scale, we observed a high correlation between the spatial patterns for precipitation variability and vegetation variability, with high precipitation variability corresponding to high vegetation variability. In addition, this study reveals increasing IAV in annual maximum vegetation in more than 45% of vegetated areas globally, whereas only 21% exhibited decreasing IAV. Regression analysis suggests that temperature changes explain the largest proportion of changes in the IAV of vegetation greenness, followed by solar radiation and precipitation.

Acknowledgments

This work was financially supported by the National Key Scientific Research and Development Program of China (grant No. 2017YFA0603601 & 2018YFC1508901) and the National Natural Science Foundation of China (grant No. 41671083).

Data availability statement

The data that support the findings of this study are openly available, and details are as follows, the GIMMS NDVI3g data set was obtained from https://ecocast.arc.nasa.gov/data/pub/gimms/3g.v1/. Global 0.5° monthly TMP and PRE data sets from 1982 to 2015 were obtained from the Climatic Research Unit Time Series 4.01 (http://data.ceda.ac.uk/badc/cru/data/cru_ts/cru_ts_4.01/). The global 0.5° monthly SWD data set for the period 1982–2015 was obtained from the Climate Research Unit—National Centers for Environmental Prediction v7 data set (http://dods.ipsl.jussieu.fr/igcmg/IGCM/BC/OOL/OL/CRU-NCEP/v5.3/halfdeg/). GPP simulations were collected from the Trends in Net Land-Atmosphere Exchange project (http://dgvm.ceh.ac.uk/). Global land cover data was obtained from MODIS (MCD12C1) (http://glcf.umd.edu/data/lc/).

All codes for data processing can be obtained by contacting the corresponding author.

ORCID iDs

Bin He https://orcid.org/0000-0002-9088-262X

References

Ahlström A, Raupach M R, Schurgers G, Smith B, Arneth A, Jung M, Reichstein M, Canadell J G, Friedlingstein P and Jain A K 2015a The dominant role of semi-arid ecosystems in the trend and variability of the land CO_2 sink *Science* **348** 895–9

Ahlström A, Xia J, Arneth A, Luo Y and Smith B 2015b Importance of vegetation dynamics for future terrestrial carbon cycling *Environ. Res. Lett.* **10** 054019

Atzberger C, Klisch A, Mattiuzzi M and Vuolo F 2013 Phenological metrics derived over the European continent from NDVI3g data and MODIS time series *Remote Sens.* **6** 257–84

Beer C, Reichstein M, Tomelleri E, Ciais P, Jung M, Carvalhais N, Rödenbeck C, Arain M A, Baldocchi D and Bonan G B 2010 Terrestrial gross carbon dioxide uptake: global distribution and covariation with climate *Science* **329** 834–81184984

Buermann W, Bikash P R, Jung M, Burn D H and Reichstein M 2013 Earlier springs decrease peak summer productivity in North American boreal forests *Environ. Res. Lett.* **8** 024027

Chen J, Jönsson P, Tamura M, Gu Z, Matsushita B and Eklundh L 2004 A simple method for reconstructing a high-quality NDVI time-series data set based on the Savitzky–Golay filter *Remote Sens. Environ.* **91** 332–44

Chen C, He B, Guo L, Zhang Y, Xie X and Chen Z 2018 Identifying critical climate periods for vegetation growth in the Northern Hemisphere *J. Geophys. Res.: Biogeosci.* **123** 2541–52

Chong I-G and Jun C-H 2005 Performance of some variable selection methods when multicollinearity is present *Chemometr. Intell. Lab. Syst.* **78** 103–12

Chun H and Keleş S 2010 Sparse partial least squares regression for simultaneous dimension reduction and variable selection *J. R. Stat. Soc.* B **72** 3–25

Cong N, Piao S, Chen A, Wang X, Lin X, Chen S, Han S, Zhou G and Zhang X 2012 Spring vegetation green-up date in China inferred from SPOT NDVI data: a multiple model analysis *Agric. Forest Meteorol.* **165** 104–13

Corlett R T 2011 Impacts of warming on tropical lowland rainforests *Trends Ecol. Evol.* **26** 606–13

Dai A 2011 Drought under global warming: a review *Wiley Interdiscip. Rev. Clim. Change* **2** 45–65

De Keersmaecker W, Lhermitte S, Tits L, Honnay O, Somers B and Coppin P 2015 A model quantifying global vegetation resistance and resilience to short-term climate anomalies and their relationship with vegetation cover *Glob. Ecol. Biogeogr.* **24** 539–48

Erasmi S, Schucknecht A, Barbosa M and Matschullat J 2014 Vegetation greenness in northeastern brazil and its relation to ENSO warm events *Remote Sens.* **6** 3041–58

Fang J, Piao S, Tang Z, Peng C and Ji W 2001 Interannual variability in net primary production and precipitation *Science* **293** 1723

Fensholt R, Langanke T, Rasmussen K, Reenberg A, Prince S D, Tucker C, Scholes R J, Le Q B, Bondeau A and Eastman R 2012 Greenness in semi-arid areas across the globe 1981–2007—an earth observing satellite based analysis of trends and drivers *Remote Sens. Environ.* **121** 144–58

Gatti R C, Di Paola A, Bombelli A, Noce S and Valentini R 2017 Exploring the relationship between canopy height and terrestrial plant diversity *Plant Ecol.* **218** 899–908

Graven H, Keeling R, Piper S, Patra P, Stephens B, Wofsy S, Welp L, Sweeney C, Tans P and Kelley J 2013 Enhanced seasonal exchange of CO_2 by northern ecosystems since 1960 *Science* **341** 1085–9

Hamed K H 2008 Trend detection in hydrologic data: the Mann–Kendall trend test under the scaling hypothesis *J. Hydrol.* **349** 350–63

Harris I, Jones P D, Osborn T J and Lister D H 2014 Updated high-resolution grids of monthly climatic observations–the CRU TS3. 10 dataset *Int. J. Climatol.* **34** 623–42

Hirota M, Holmgren M, Van Nes E H and Scheffer M 2011 Global resilience of tropical forest and savanna to critical transitions *Science* **334** 232–5

Holben B N 1986 Characteristics of maximum-value composite images from temporal AVHRR data *Int. J. Remote Sens.* **7** 1417–34

Hoover D L, Knapp A K and Smith M D 2014 Resistance and resilience of a grassland ecosystem to climate extremes *Ecology* **95** 2646–56

Huang L, He B, Chen A, Wang H, Liu J, Lǚ A and Chen Z 2016 Drought dominates the interannual variability in global terrestrial net primary production by controlling semi-arid ecosystems *Sci. Rep.* **6** 24639

Hu Z, Shi H, Cheng K, Wang Y P, Piao S, Li Y, Zhang L, Xia J, Zhou L and Yuan W 2018 Joint structural and physiological control on the interannual variation in productivity in a temperate grassland: a data-model comparison *Glob. Change Biol.* **24** 2965–79

Humphrey V, Zscheischler J, Ciais P, Gudmundsson L, Sitch S and Seneviratne S I 2018 Sensitivity of atmospheric CO_2 growth rate to observed changes in terrestrial water storage *Nature* **560** 628

Iio A, Hikosaka K, Anten N P, Nakagawa Y and Ito A 2014 Global dependence of field-observed leaf area index in woody species on climate: a systematic review *Glob. Ecol. Biogeogr.* **23** 274–85

IPCC 2007 *Climate Change 2007: the Physical Science Basis Contribution of Working Group I to The Fourth Assessment Report of the Intergovermental Panel on Climate Change* ed F Stocker *et al* (Cambridge: Cambridge University Press)

IPCC 2013 *Climate Change 2013: the Physical Science Basis: Working Group I Contribution to the Fifth Assessment Report of the Intergovernmental Panel on Climate Change* (Cambridge: Cambridge University Press)

Jönsson P and Eklundh L 2004 TIMESAT—a program for analyzing time-series of satellite sensor data *Comput. Geosci.* **30** 833–45

Jakubauskas M E, Legates D R and Kastens J H 2001 Harmonic analysis of time-series AVHRR NDVI data *Photogramm. Eng. Remote Sens.* **67** 461–70

Jiang N, Zhu W, Zheng Z, Chen G and Fan D 2013 A comparative analysis between GIMSS NDVIg and NDVI3g for monitoring vegetation activity change in the northern hemisphere during 1982–2008 *Remote Sens.* **5** 4031–44

Jiang C, Ryu Y, Fang H, Myneni R, Claverie M and Zhu Z 2017 Inconsistencies of interannual variability and trends in long-term satellite leaf area index products *Glob. Change Biol.* **23** 4133–46

Jolliffe I T 1982 A note on the use of principal components in regression *Appl. Stat.* 300–3

Julien Y and Sobrino J 2009 Global land surface phenology trends from GIMMS database *Int. J. Remote Sens.* **30** 3495–513

Keenan T F, Prentice I C, Canadell J G, Williams C A, Wang H, Raupach M and Collatz G J 2016 Recent pause in the growth rate of atmospheric CO_2 due to enhanced terrestrial carbon uptake *Nat. Commun.* **7** 13428

Knapp A K and Smith M D 2001 Variation among biomes in temporal dynamics of aboveground primary production *Science* **291** 481–4

Knorn J, Rabe A, Radeloff V C, Kuemmerle T, Kozak J and Hostert P 2009 Land cover mapping of large areas using chain classification of neighboring Landsat satellite images *Remote Sens. Environ.* **113** 957–64

Kottek M, Grieser J, Beck C, Rudolf B and Rubel F 2006 World Map of the Köppen-Geiger climate classification updated *Meteorol. Z.* **15** 259–63

Le Hourou H, Bingham R and Skerbek W 1988 Relationship between the variability of primary production and the variability of annual precipitation in world arid lands *J. Arid. Environ.* **15** 1–18

Lioubimtseva E and Henebry G M 2009 Climate and environmental change in arid Central Asia: impacts, vulnerability, and adaptations *J. Arid. Environ.* **73** 963–77

Liu G, Liu H and Yin Y 2013 Global patterns of NDVI-indicated vegetation extremes and their sensitivity to climate extremes *Environ. Res. Lett.* **8** 025009

Liu Y Y, van Dijk A I, Miralles D G, McCabe M F, Evans J P, de Jeu R A, Gentine P, Huete A, Parinussa R M and Wang L 2018 Enhanced canopy growth precedes senescence in 2005 and 2010 Amazonian droughts *Remote Sens. Environ.* **211** 26–37

Mann H B 1945 Nonparametric tests against trend *Econometr.: J. Econometr. Soc.* **13** 245–59

McDowell N G and Allen C D 2015 Darcy's law predicts widespread forest mortality under climate warming *Nat. Clim. Change* **5** 669

Mehmood T, Liland K H, Snipen L and Sæbø S 2012 A review of variable selection methods in partial least squares regression *Chemometr. Intell. Lab. Syst.* **118** 62–9

Morton D C, Nagol J, Carabajal C C, Rosette J, Palace M, Cook B D, Vermote E F, Harding D J and North P R 2014 Amazon forests maintain consistent canopy structure and greenness during the dry season *Nature* **506** 221

Nemani R R, Keeling C D, Hashimoto H, Jolly W M, Piper S C, Tucker C J, Myneni R B and Running S W 2003 Climate-driven increases in global terrestrial net primary production from 1982 to 1999 *Science* **300** 1560–3

Osborne T M and Wheeler T R 2013 Evidence for a climate signal in trends of global crop yield variability over the past 50 years *Environ. Res. Lett.* **8** 024001

Pan Y, Birdsey R A, Fang J, Houghton R, Kauppi P E, Kurz W A, Phillips O L, Shvidenko A, Lewis S L and Canadell J G 2011 A large and persistent carbon sink in the world's forests *Science* **1201609**

Perkins S, Alexander L and Nairn J 2012 Increasing frequency, intensity and duration of observed global heatwaves and warm spells *Geophys. Res. Lett.* **39** L20714

Phillips O L, Aragão L E, Lewis S L, Fisher J B, Lloyd J, López-González G, Malhi Y, Monteagudo A, Peacock J and Quesada C A 2009 Drought sensitivity of the Amazon rainforest *Science* **323** 1344–7

Piao S, Fang J, Zhou L, Zhu B, Tan K and Tao S 2005 Changes in vegetation net primary productivity from 1982 to 1999 in China *Glob. Biogeochem. Cycles* **19** GB2027

Piao S, Nan H, Huntingford C, Ciais P, Friedlingstein P, Sitch S, Peng S, Ahlström A, Canadell J G and Cong N 2014 Evidence for a weakening relationship between interannual temperature variability and northern vegetation activity *Nat. Commun.* **5** 5018

Piao S, Tan J, Chen A, Fu Y H, Ciais P, Liu Q, Janssens I A, Vicca S, Zeng Z and Jeong S-J 2015 Leaf onset in the northern hemisphere triggered by daytime temperature *Nat. Commun.* **6** 6911

Piao S, Liu Z, Wang T, Peng S, Ciais P, Huang M, Ahlstrom A, Burkhart J F, Chevallier F and Janssens I A 2017 Weakening temperature control on the interannual variations of spring carbon uptake across northern lands *Nat. Clim. Change* **7** 359–63

Poulter B, Frank D, Ciais P, Myneni R B, Andela N, Bi J, Broquet G, Canadell J G, Chevallier F and Liu Y Y 2014 Contribution of semi-arid ecosystems to interannual variability of the global carbon cycle *Nature* **509** 600

Propastin P, Fotso L and Kappas M 2010 Assessment of vegetation vulnerability to ENSO warm events over Africa *Int. J. Appl. Earth Obs. Geoinf.* **12** S83–9

Ray D K, Mueller N D, West P C and Foley J A 2013 Yield trends are insufficient to double global crop production by 2050 *PLoS One* **8** e66428

Ray D K, Gerber J S, MacDonald G K and West P C 2015 Climate variation explains a third of global crop yield variability *Nat. Commun.* **6** 5989

Reichstein M, Bahn M, Ciais P, Frank D, Mahecha M D, Seneviratne S I, Zscheischler J, Beer C, Buchmann N and Frank D C 2013 Climate extremes and the carbon cycle *Nature* **500** 287

Reidsma P, Ewert F, Lansink A O and Leemans R 2010 Adaptation to climate change and climate variability in European agriculture: the importance of farm level responses *Eur. J. Agron.* **32** 91–102

Richardson A D, Black T A, Ciais P, Delbart N, Friedl M A, Gobron N, Hollinger D Y, Kutsch W L, Longdoz B and Luyssaert S 2010 Influence of spring and autumn phenological transitions on forest ecosystem productivity *Phil. Trans. R. Soc.* B **365** 3227–46

Rouse J W, Haas R H, Schell J and Deering D 1973 Monitoring the vernal advancement and retrogradation (green wave effect) of natural vegetation *Technical Report NAS5-21857* NASA (https://ntrs.nasa.gov/archive/nasa/casi.ntrs.nasa.gov/19730017588.pdf)

Samanta A, Ganguly S, Hashimoto H, Devadiga S, Vermote E, Knyazikhin Y, Nemani R R and Myneni R B 2010 Amazon forests did not green-up during the 2005 drought *Geophys. Res. Lett.* **37** L05401

Schucknecht A, Erasmi S, Niemeyer I and Matschullat J 2013 Assessing vegetation variability and trends in north-eastern Brazil using AVHRR and MODIS NDVI time series *Eur. J. Remote Sens.* **46** 40–59

Seddon A W, Macias-Fauria M, Long P R, Benz D and Willis K J 2016 Sensitivity of global terrestrial ecosystems to climate variability *Nature* **531** 229–32

Sen P K 1968 Estimates of the regression coefficient based on Kendall's tau *J. Am. Stat. Assoc.* **63** 1379–89

Silva C E, Kellner J R, Clark D B and Clark D A 2013 Response of an old-growth tropical rainforest to transient high temperature and drought *Glob. Change Biol.* **19** 3423–34

Sitch S, Friedlingstein P, Gruber N, Jones S, Murray-Tortarolo G, Ahlström A, Doney S C, Graven H, Heinze C and Huntingford C 2015 Recent trends and drivers of regional sources and sinks of carbon dioxide *Biogeosciences* **12** 653–79

Sloat L L, Gerber J S, Samberg L H, Smith W K, Herrero M, Ferreira L G, Godde C M and West P C 2018 Increasing importance of precipitation variability on global livestock grazing lands *Nat. Clim. Change* **8** 214

Smith A M, Kolden C A, Tinkham W T, Talhelm A F, Marshall J D, Hudak A T, Boschetti L, Falkowski M J, Greenberg J A and Anderson J W 2014 Remote sensing the vulnerability of vegetation in natural terrestrial ecosystems *Remote Sens. Environ.* **154** 322–37

Sulman B N, Roman D T, Yi K, Wang L, Phillips R P and Novick K A 2016 High atmospheric demand for water can limit forest carbon uptake and transpiration as severely as dry soil *Geophys. Res. Lett.* **43** 9686–95

Thornton P K, Ericksen P J, Herrero M and Challinor A J 2014 Climate variability and vulnerability to climate change: a review *Glob. Change Biol.* **20** 3313–28

Wang W, Ciais P, Nemani R R, Canadell J G, Piao S, Sitch S, White M A, Hashimoto H, Milesi C and Myneni R B 2013 Variations in atmospheric CO_2 growth rates coupled with tropical temperature *Proc. Natl Acad. Sci.* **110** 13061–6

Wang X, Piao S, Ciais P, Friedlingstein P, Myneni R B, Cox P, Heimann M, Miller J, Peng S and Wang T 2014 A two-fold increase of carbon cycle sensitivity to tropical temperature variations *Nature* **506** 212

Wu D, Zhao X, Liang S, Zhou T, Huang K, Tang B and Zhao W 2015 Time-lag effects of global vegetation responses to climate change *Glob. Change Biol.* **21** 3520–31

Wu M, Schurgers G, Rummukainen M, Smith B, Samuelsson P, Jansson C, Siltberg J and May W 2016 Vegetation-climate feedbacks modulate rainfall patterns in Africa under future climate change *Earth Syst. Dyn.* **7** 627–47

Xu L, Samanta A, Costa M H, Ganguly S, Nemani R R and Myneni R B 2011 Widespread decline in greenness of Amazonian vegetation due to the 2010 drought *Geophys. Res. Lett.* **38** L07402

Yang Y, Guan H, Batelaan O, McVicar T R, Long D, Piao S, Liang W, Liu B, Jin Z and Simmons C T 2016 Contrasting responses of water use efficiency to drought across global terrestrial ecosystems *Sci. Rep.* **6** 23284

Yuan W, Piao S, Qin D, Dong W, Xia J, Lin H and Chen M 2018 Influence of vegetation growth on the enhanced seasonality of atmospheric CO_2 *Glob. Biogeochem. Cycles* **32** 32–41

Yue S, Pilon P, Phinney B and Cavadias G 2002 The influence of autocorrelation on the ability to detect trend in hydrological series *Hydrol. Process.* **16** 1807–29

Zeng F-W, Collatz G J, Pinzon J E and Ivanoff A 2013 Evaluating and quantifying the climate-driven interannual variability in global inventory modeling and mapping studies (GIMMS) normalized difference vegetation index (NDVI3g) at global scales *Remote Sens.* **5** 3918–50

Zhang Y, Zhu Z, Liu Z, Zeng Z, Ciais P, Huang M, Liu Y and Piao S 2016 Seasonal and interannual changes in vegetation activity of tropical forests in Southeast Asia *Agric. Forest Meteorol.* **224** 1–10

Zhao L, Dai A and Dong B 2018 Changes in global vegetation activity and its driving factors during 1982–2013 *Agric. Forest Meteorol.* **249** 198–209

Zhu Z, Bi J, Pan Y, Ganguly S, Anav A, Xu L, Samanta A, Piao S, Nemani R and Myneni R 2013 Global data sets of vegetation leaf area index (LAI) 3g and fraction of photosynthetically active radiation (FPAR) 3g derived from global inventory modeling and mapping studies (GIMMS) normalized difference vegetation index (NDVI3g) for the period 1981 to 2011 *Remote Sens.* **5** 927–48

Zhu Z, Piao S, Myneni R B, Huang M, Zeng Z, Canadell J G, Ciais P, Sitch S, Friedlingstein P and Arneth A 2016 Greening of the Earth and its drivers *Nat. Clim. Change* **6** 791–5